On-Surface Synthesis of Phthalocyanine Compounds

E. Nardi, M. Koudia, S. Kezilebieke, J.-P. Bucher and M. Abel

Abstract In this chapter, we review the recent progress in the synthesis of phthalocyanine compounds at metallic surfaces under ultra-high vacuum conditions. Starting with tetra-carbonitrile-benzene molecules and magnetic atoms such as iron and manganese, we show that metal–organic coordination networks are formed at room temperature; then annealing at 500–600 K leads to the on-surface formation of phthalocyanine compounds. This reaction has been studied step-by-step by scanning tunneling microscopy and spectroscopy. The last part of this chapter is dedicated to the study of larger precursors functionalized with tetra-carbonitrile groups that react with copper atoms to form original polymers linked by phthalocyanine cores.

1 Introduction

Among technologically relevant molecules for organic electronic devices, the metallophthalocyanines (MPc) are very extensively studied for their chemical and optoelectronic properties [1]. They can be employed as building blocks for a wide range of applications such as gas sensors, field effect transistors, organic light emitting diodes, or data storage devices. The polymeric forms of phthalocyanines have been known for a long time [2–7] but the isolation of single sheet of 2D

E. Nardi · M. Koudia · M. Abel (✉)
Institut Matériaux, Microélectronique et Nanosciences de Provence, CNRS UMR7334, Aix Marseille Université, Marseille 13397, France
e-mail: mathieu.abel@im2np.fr

E. Nardi
e-mail: elena.nardi@im2np.fr

S. Kezilebieke · J.-P. Bucher
Université de Strasbourg, Institut Universitaire de France, 23 rue du Loess, Strasbourg 67034, France
e-mail: jean-pierre.bucher@ipcms.unistra.fr

A. Gourdon (ed.), *On-Surface Synthesis*, Advances in Atom and Single Molecule Machines, DOI 10.1007/978-3-319-26600-8_6

polymer has never been obtained. One of the main interests is the combination of magnetic properties given by the central metals with pi-conjugated electrons of phthalocyanines. The molecular magnetism arises from the unpaired spins residing in the *d*-orbitals of the atom. Such molecules adsorbed on metallic substrates have recently gained special interest in view of emerging field of spintronics and spin-based devices. Preparation of supramolecular assemblies at surfaces under ultra-high vacuum (UHV) conditions usually requires deposition of the molecular building blocks by thermal sublimation from a crucible. Therefore, there is a limit to the weight of molecular building blocks that can be utilized in these studies: the high temperature required for their evaporation leads to thermal decomposition or to polymerization in the crucible before evaporation. A possible approach to the problem is to use smaller molecular precursors which react with atoms on the surface and form phthalocyanine compounds (Scheme 1).

Density functional theory (DFT) calculations predict very interesting properties for polymeric phthalocyanine (Table 1) [8]. Series of magnetic atoms have been theoretically studied and it appears that only Mn has a ferromagnetic coupling, whereas the coupling of the other metals is antiferromagnetic. However, the most important behavior is a high exchange energy in case of Mn (E_{ex} = 125 meV) accompanied by a half-metallic character. This gives hope for remarkable properties for the development of materials for spintronic applications.

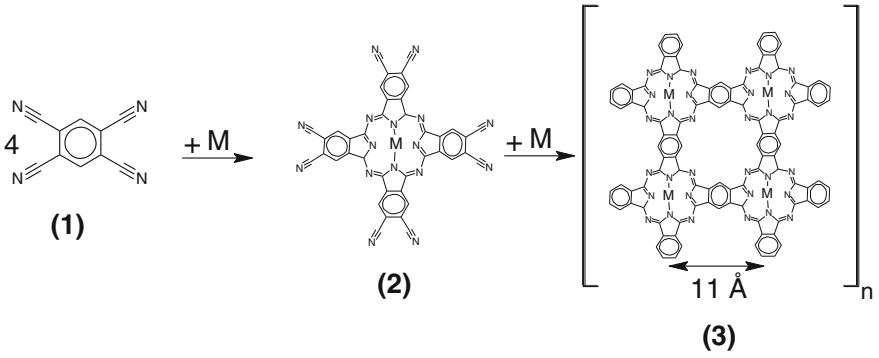

Scheme 1 Schematic diagram of the reaction between tetra-carbonitrile benzene (TCNB) molecules (**1**) and metallic atoms to form octacyano metallophthalocyanine (**2**) when the reaction goes on, it can form the polymeric–phthalocyanine compound (**3**) [1]

Table 1 Density functional theory calculations in the framework LDA + U of the magnetic configuration of the 2D polymers

	Cr	Mn	Fe	Co	Ni	Cu	Zn
E_{ex}	−29	124	−14	−6	–	−7	–
M	4	3	2	1	0	1	0
E_g	0.36	Half-metal	0.24	0.10	0.34	0.31	0.30

E_{ex} Exchange energy per supercell (E_{ex} in meV); total magnetic moment per supercell (M in μB), and energy band gap (E_g in eV) Ref. [8]

In the first part of this chapter, the possibility to induce surface reactions between small ligands—tetra-carbonitrile benzene (TCNB)—and magnetic atoms (Scheme 1) is demonstrated. This is done by depositing metallic atoms (Fe or Mn) and TCNB molecules under UHV conditions. At room temperature, TCNB molecules form large metal–organic networks with both Fe and Mn atoms in 1:4 and 1:2 stoichiometries [9–11]. For the reaction to occur, it is necessary to heat the surface to 500–550 K [12, 13]. At these temperatures, a significant proportion of molecules desorbs from the surface, necessitating a fine tuning between reaction and desorption. Since the Mn is slightly more reactive than Fe, the reaction evolves more efficiently in the former case, leading to comparatively larger MnPc domains. Further activation at higher annealing temperatures then leads to the formation of small domains of polymeric Mn-phthalocyanine.

In the second part of this chapter, it is shown on the example of Fe-TCNB that low-temperature, high-resolution scanning tunneling spectroscopy (STS) provides a powerful identification of the step-by-step evolution of the chemical reaction. In particular, a deeper insight into the genesis of the magnetic properties of such compounds is achieved. A good illustration of the convergence toward the covalent properties is the emergence of the Kondo resonance in FePc.

The last part of this chapter describes the potentiality and versatility of this method to access to a diversity of hybrid organic–inorganic compounds. New molecular precursors functionalized by tetra-carbonitrile groups are used in combination with copper atoms to form original 1D and 2D polymers linked by phthalocyanine cores. In that case, the homogeneity of the reaction allows full conclusive X-ray photoelectron spectroscopy (XPS) measurements of the chemical reaction [14].

2 Reaction Between Tetra-Carbonitrile Benzene and Magnetic Atoms (Fe or Mn)

In this example, the stepwise identification of the reaction between molecular TCNB and atomic Fe toward the final FePc product is achieved. The self-assembly of the vapor deposited TCNB molecules and Fe atoms on Au(111) first leads to tetra-coordinated $Fe(TCNB)_4$ and $Fe(TCNB)_2$ precursors [9]. However, among the two tetra-coordinate phases, only the $Fe(TCNB)_2$ network has the appropriate stoichiometry for the synthesis of FePc on Au(111). This phase is composed of Fe atoms interconnected with TCNB molecules (Fig. 1a, b) [12]. Large homochiral and mirror symmetric $Fe(TCNB)_2$ domains with a lateral extension up to 50 nm are present on the surface (Fig. 1a). It is worth mentioning that a similar result is obtained on Ag(100), indicating that the coordination network is relatively insensitive to the surface template, i.e., to the crystallography and, to some extent, to the chemical nature of the underlying substrate. A careful analysis of the STM data shows that the $Fe(TCNB)_2$ network has a square structure with a measured periodicity of 1.15 ± 0.1 nm in both orthogonal directions (Fig. 1b). The unit cell of the

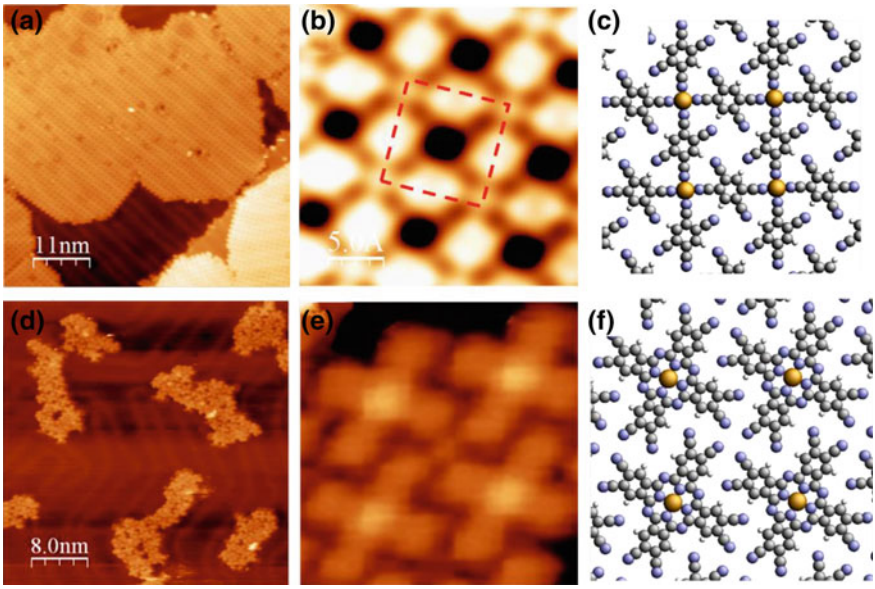

Fig. 1 STM topography images. **a**, **b** $Fe(TCNB)_2$ network on Au(111) acquired at $I = 0.2$ nA and $V = -0.9$ V. **c**, **d** Units of $FePc(CN)_8$ on Au(111), obtained upon annealing the previous Fe $(TCNB)_2$ structure at 550 K, acquired at $I = 1.8$ nA and $V = -0.9$ V. **e**, **f** Corresponding schematics. Adapted with permission from Ref. [12]. Copyright 2014 American Chemical Society

$Fe(TCNB)_2$ network (Fig. 1b, c) contains eight nitrogen atoms, four of which having a coordination bond with one single Fe atom. Annealing the $Fe(TCNB)_2$ phase to 550 K leads to the formation of cross-like molecules of octacyano-FePc ($FePc(CN)_8$) (Fig. 1e, f). The Fe atoms appear as bright protrusions (Fig. 2f), confirming the presence of d_{z2} orbitals of Fe while the organic ligands appear as four symmetric lobes. Full transformation into covalent bonds is further ascertained from the absence of chirality of the ligands around the central metal.

The annealing used for the reaction between Fe and TCNB at 550 K produces large desorption of the molecules and dilution of the metallic atoms into the substrate. In that case, the reaction has a limited yield and it results in small domains of iron phthalocyanine. Using manganese instead of iron atoms for the reaction with TCNB molecules allows a modification of the reaction efficiency because Mn, which has a less filled *d*-band than Fe, is more reactive. The room temperature phase obtained with Mn and TCNB (Fig. 2a) is very similar to the room temperature phase previously obtained with Fe and TCNB. Its annealing at 370 K allows the activation of the reaction and the formation of a Mn-phthalocyanine (Mn-Pc) network linked by hydrogen bonding (Fig. 2b). Additional Mn atoms can be found between the Mn-Pc (dotted circle in Fig. 2c) coordinating half of the available carbonitrile groups. Using the same STM tip is now possible to distinguish two electronic behaviors of Mn atoms: Mn in the cross-like compounds (solid line circles) that appears 0.4 Å above the molecular plane while Mn in between the

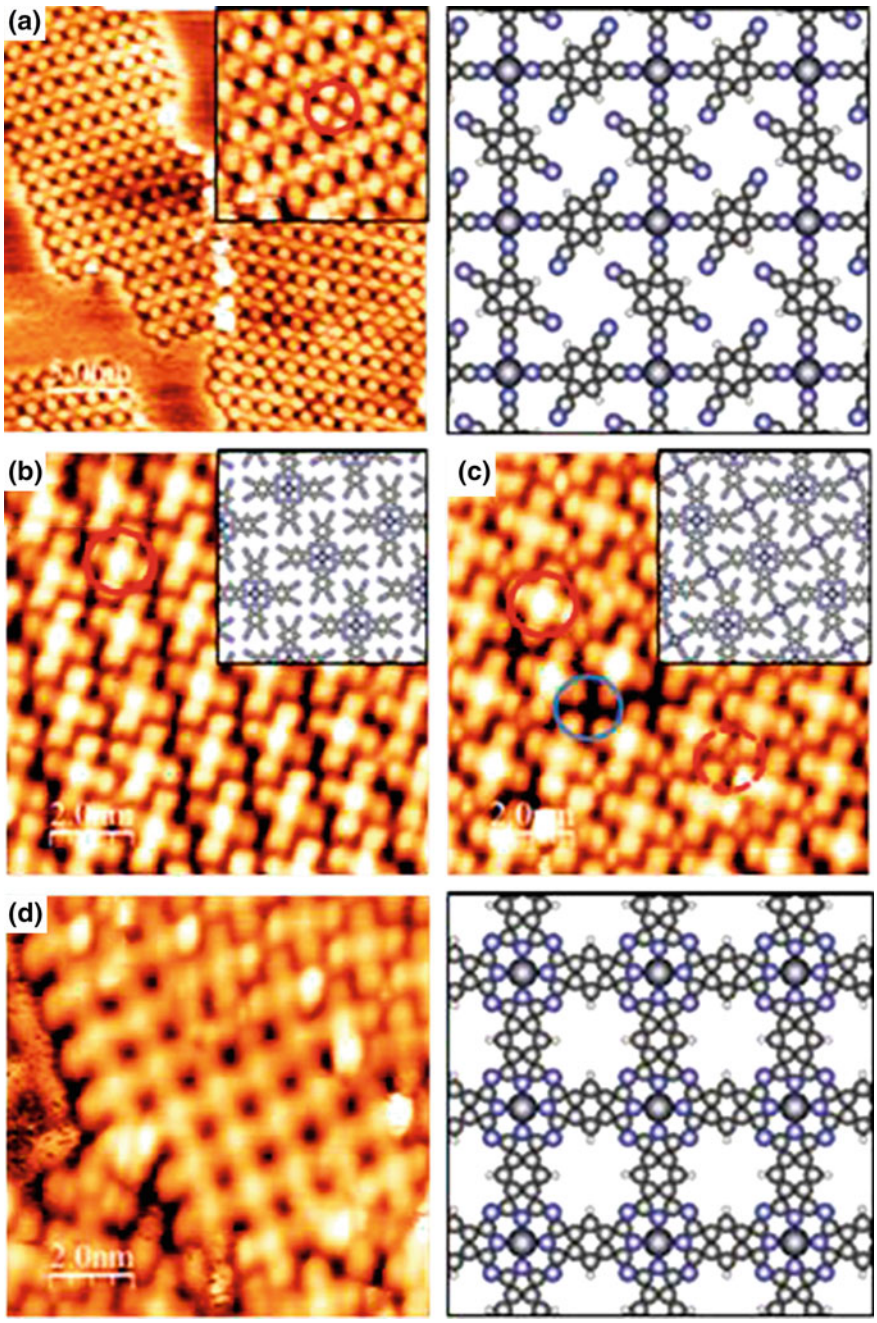

Fig. 2 STM topography images. **a** $Mn(TCNB)_2$ networks on Ag(111); **b** $MnPc(CN)_8$ on Ag(111) obtained after annealing at 370 K linked by hydrogen bonding **c** $MnPc(CN)_8$ obtained after annealing at 370 K linked by metal–ligand interactions; **d** Polymeric form of the MnPc obtained after annealing at 500 K. Adapted from Ref. [13] with permission from The Royal Society of Chemistry

Mn–Pcs (dotted line circle) that appears 0.1 Å lower. The temperature needs to be increased up to 500 K for the reaction to proceed further and to form small domains of polymeric Mn-phthalocyanines (Fig. 2d).

2.1 STS Identification of Chemical Bonds During the Synthesis of Fe-Phthalocyanine on Au(111)

Scanning tunneling spectroscopy has become a key tool to access properties of metal–organic molecules adsorbed on surfaces. In this context, the MPc's have been extensively studied due to their advantageous face-on adsorption providing easy access to metal atoms and ligands with the STM probe tip [15–22]. STS has been applied on FePc on Au(111) to track the covalent self-assembly of organic ligands and metal atoms [12]. The STS characterization of $FePc(CN)_8$ complexes reveals a strong similarity with the results obtained for FePc in the literature. This comes from a small influence of the peripheral functionalization (CN instead of H) on the orbital configuration of Fe atom. Thus, magnetic moment and spin state are expected to be the same in both systems which are further ascertained by comparing the projected density of states (PDOS) calculations for both systems [12].

To get a deeper insight into the hierarchy of chemical bonding of the iron atom, STS measurements on the freshly deposited FePc on Au(111) have been compared with those of the $Fe(TCNB)_2$ phase on Au(111) [12]. The measurements were performed in a low-temperature STM operating at a temperature of 4.6 K and UHV conditions. Two dI/dV spectra taken above the Fe atom (red) and on the benzene rings (black) of a FePc molecule are presented in Fig. 3 (upper panels). There are seven main features at sample bias of −0.9, −0.79, −0.72, −0.37, −0.17, +0.5, and 0 V. Relevant features in the dI/dV spectra are only expected when a significant overlap between tip states and molecular orbitals is achieved. This is possible for example in the case of d_{z2}, d_{xz}, and d_{yz} orbitals above the Fe atom. The sharp peak labeled No. 1 (Fig. 3) and located at −0.9 V corresponds to the lower occupied molecular orbital (HOMO-1) while the shoulder at −0.79 V (No. 2) has been attributed to the $d_{xz/yz}$ orbitals of iron [16]. The peak at −0.72 V (No. 3) on the ligand is attributed to the HOMO which is in good agreement with valence-band photoemission studies on FePc/Au(111) [23]. The relatively intense resonance at −0.38 V (labeled No. 4) is similar to the one observed by Gao et al. [16] most probably arising from the hybridization of the Fe atom in the FePc molecule with the Au(111) electronic surface state. Such surface-induced states (Fig. 3b labeled SI) have been observed for FePc on other substrates and are quite common for atoms on noble metal surfaces [20, 22]. The peak located at −0.17 V (No. 5) was not reported in the previous studies of FePc on Au(111) although a similar feature has been observed for FePc on Ag(100) [22] and Ag(111) [17] surfaces. The peak close to the Fermi level (No. 6) is a well-known Kondo signature previously observed in FePc on Au(111) [16, 21]. Additional information on the spatial

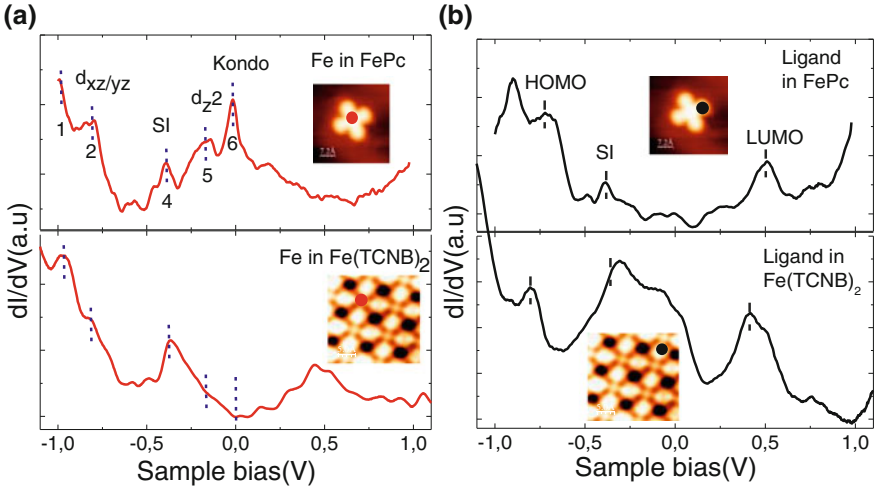

Fig. 3 Comparison of d*I*/d*V* spectra taken on the $Fe(TCNB)_2$ network and on the FePc molecule on Au(111) under the same conditions (feedback loop opened at $V = -0.7$ V, $I = 0.2$ nA). **a** d*I*/d*V* spectra taken above the Fe in FePc and in $Fe(TCNB)_2$, respectively, **b** d*I*/d*V* taken above the ligands of $Fe(TCNB)_2$ and above the lobes of FePc, respectively. Adapted with permission from Ref. [12]. Copyright 2014 American Chemical Society

distribution of the molecular orbitals can be obtained by recording the constant-height differential conductance (d*I*/d*V*) maps at different bias voltages [12, 18], thus providing information on dominant conduction channels above the molecules. Thereby, it was confirmed that the localized contrast associated with peak No. 5 and No. 6 in the d*I*/d*V* maps both originates from out-of-plane d_{z2} state of the Fe atom [12].

Although each Fe atom in the $Fe(TCNB)_2$ phase has four neighbor nitrogens as in the FePc molecule, the spectra in both systems show significant differences but also remarkable similarities. The differences mainly come from different chemical bonding between Fe and ligands: from metal–ligand interactions in $Fe(TCNB)_2$ to covalent bonds in FePc. Figure 3 shows d*I*/d*V* spectra for both $Fe(TCNB)_2$ and FePc with the STM tip above the Fe atom (Fig. 3a) and above the ligand (Fig. 3b). The two systems show three similar features: two similarities are observed on the Fe atom and one on the ligand. In particular, the feature at −0.79 V on the Fe, attributed to the d_π (d_{xz} and d_{yz}) orbitals, is similar in both systems indicating that the Fe has a similar environment in the two cases. The second remarkable feature is the surface-induced state (No. 4 in Fig. 3a) found above the Fe atom at −0.38 V indicating that Fe atom has the same influence on the Au(111) sp surface state. The spectra acquired on the ligand (Fig. 3b) show that both LUMO and HOMO of $Fe(TCNB)_2$ and FePc appear at the same energy (+0.50 V and −0.72 eV, respectively). These similarities are summarized in Table 2.

The presence of a Kondo resonance for FePc on Au(111) (No. 6 in Fig. 3a) with a corresponding Kondo temperature of about 200 K deserves a special attention as it

Table 2 Summary of the similar peak positions for FePc and $Fe(TCNB)_2$ on Au (111) given in eV

	No.	FePc	$Fe(TCNB)_2$
$d_{xz/yz}$	2	−0.79	−0.79
HOMO	3	−0.72	−0.76
SI	4	−0.38	−0.38
d_{z2}	5	−0.17	–
Kondo	6	Yes	No
LUMO	7	+0.5	+0.5

Ref. [12]

disappears in $Fe(TCNB)_2$. In FePc, the oxidation state of the iron is Fe(II) with the electronic configuration $(d_{xy})^2$, $(d_{z2})^1$, $(d_\pi)^3$ inducing a spin $S = 1$. The fact that the Kondo resonance of FePc/Au(111) is located at the metal ion can be related to a screened Kondo spin originating from the d_{z2} orbital (local moment Kondo system). This result is far from being trivial since on similar MPc systems (adsorbed on noble metals) the maximum of the Kondo resonance intensity was found on the ligands, arising from unpaired spins in the d_π orbital [22]. It is also in contrast to the fully delocalized Kondo resonance observed over the Co-porphyrin molecules on Cu(111) [24]. Finally, the above result related to the Kondo resonance of FePc by Kezilebieke et al. is in good agreement with the work of Minamitani et al. [21] who found that for FePc on Au(111) the strong coupling of the d_{z2} orbital overcomes the zero-field splitting providing a temperature window where the Kondo screening becomes dominant (effective Hamiltonian with $S = 1/2$). The partial screening of the $S = 1$ spin of FePc was also reported by Stepanow et al. [25]. To evaluate the hybridization of the Fe d_{z2} state with the substrate, STS measurements were carried out on FePc adsorbed on Au(111), Cu(111), and a cobalt nano-island [12]. The corresponding d*I*/d*V* spectra exhibit an increasing shift of the Fe *d*-state toward the Fermi level. The positions of the Fe *d*-states are summarized in Table 3 for different surfaces.

The *d*-states shift over the Fe is rationalized by means of the *d*-band model [26, 27] whose key parameter is the position of the *d*-band center with respect to the Fermi energy. As shown in Table 3, the *d*-state shift follows the same order as the *d*-band filling and the *d*-band center position: Ag < Au < Cu < Co. As a result, in case of Ag where the *d*-band center is lower in energy, the interaction with adsorbates gives rise to a large fraction of antibonding states which results in the lower adsorption energy. On the contrary, the Co surface has a *d*-band center close to the Fermi level. A large fraction of the antibonding states between the adsorbate and the surface is pushed above the Fermi level resulting in the higher adsorption energy. This might explain the strong Fe *d*-states shift observed for FePc adsorbed on the cobalt nano-islands. Experimental results for FePc molecules and Fe $(TCNB)_2$ complexes are in good agreement with DFT calculations [12]. The

Table 3 Positions of the d_{z2} resonance of Fe for FePc molecules adsorbed on metallic surfaces

	Ag(111)	Ag(100)	Au(111)	Cu(111)	Co island
Peak position (mV)	−250	−250	−170	−50	−10

Refs. [12, 17, 22]

calculation for the $Fe(TCNB)_2$ complex shows that the broad peak in the STS spectrum at +0.5 eV corresponds to an empty d_{z2} state, whereas FePc shows an occupied d_{z2} resonance just below the Fermi level. Therefore, the lack of Kondo signature for $Fe(TCNB)_2$ cannot be ascribed to a different Fe-substrate distance and is most probably due to the intrinsic differences mentioned above. As expected, the calculation clearly shows a localized spin density on the Fe of FePc with $S = 1$, whereas $Fe(TCNB)_2$ shows a weekly delocalized spin density on the ligand with Fe bearing only a fraction ($S = 0.68$) of the total spin [12].

In conclusion, the information gathered from high-resolution d*I*/d*V* spectroscopic labeling and spin-polarized DFT calculations shows that the d_π features appear already on the intermediate $Fe(TCNB)_2$ complex. The contribution of the covalent character of the surface-synthesized FePc is evidenced by the appearance of the d_{z2} state close to the Fermi energy and the related Kondo resonance, as demonstrated by studying the hybridization of the d_{z2} orbital of Fe to various substrates (Cu, Au, and Co) by STS. The lack of Kondo resonance in $Fe(TCNB)_2$ is related to the absence of the d_{z2} feature just below E_F and appears to be intrinsic to the complex.

2.2 *Reaction Between Pyrazino Phenanthroquinoxaline-Tetracarbonitrile and Copper Atoms*

Here, we show that a copper-phthalocyanine derivative is synthesized at the surface from a larger organic component, the pyrazino phenanthroquinoxaline-tetracarbonitrile (PPCN) (Scheme 2). The tunability of the electronic and structural properties of phthalocyanines makes this class of molecules ideal for both

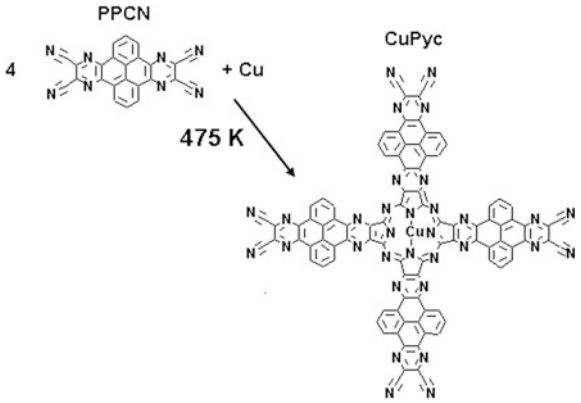

Scheme 2 Reaction between pyrazino phenanthroquinoxaline-tetracarbonitrile (PPCN) and copper atoms leading to octacyano-copper pyrenopyrazinocyanines (CuPycs)

fundamental science and technological applications, such as optoelectronic devices, sensors, and thin-film transistors.

PPCN was sublimated from a crucible onto a clean Au(111) surface. Submonolayer deposition of PPCN at room temperature in UHV results in the formation of well-ordered two-dimensional molecular domains extended over entire terraces and stabilized by weak interactions. Electron beam evaporator was used to deposit Cu atoms on top of the PPCN layer. After annealing at T = 355 K, well-ordered regular structures, in which metal centers connect to organic molecules, emerge in domains up to 120 nm in size [14].

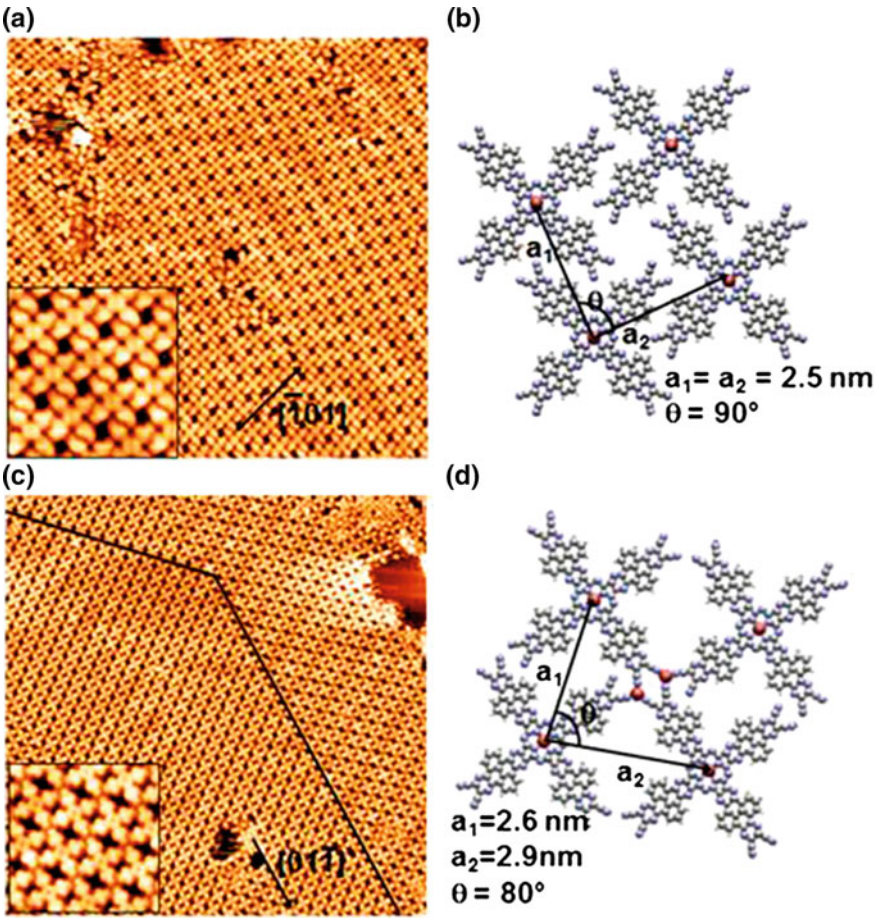

Fig. 4 Copper pyrenopyrazinocyanine (CuPyc) networks. **a** STM image (50 × 50 nm^2) of CuPycs linked by C–N···H–C bonds. *Inset* zoom (1.8 × 1.8 nm^2). **b** DFT model of the CuPyc network. **c** STM image (80 × 80 nm^2) showing the CuPycs linked by metal–organic interactions. Two mirror domains are present, separated by the *black line*. *Inset* zoom (2 × 2 nm^2). **d** DFT model of the CuPyc network linked by metal–ligand interaction. Adapted with permission from Ref. [14]. Copyright 2014 American Chemical Society

The phthalocyanine network (Fig. 4a–d) is obtained upon annealing at 475 K: the PPCN molecules react with Cu atoms to form new macromolecules derived from phthalocyanines (CuPyc, Copper pyrenopyrazinocyanine). Deposition of Cu atoms on this layer results in an extended coordination network, with domains up to 100 nm in size, in which each Cu atom is coordinated to three CuPycs (Fig. 4c). Finally, the increase in annealing temperature to 540 and 675 K leads to the formation of 1D and 2D phthalocyanine polymers, respectively (Fig. 5a–d).

An ultimate proof of the reaction between copper and PPCN is given by XPS core-level measurements of the different elements (C, N, and Cu) in the molecular film [14]. The modification of the shape of the C1s photoemission spectrum as a

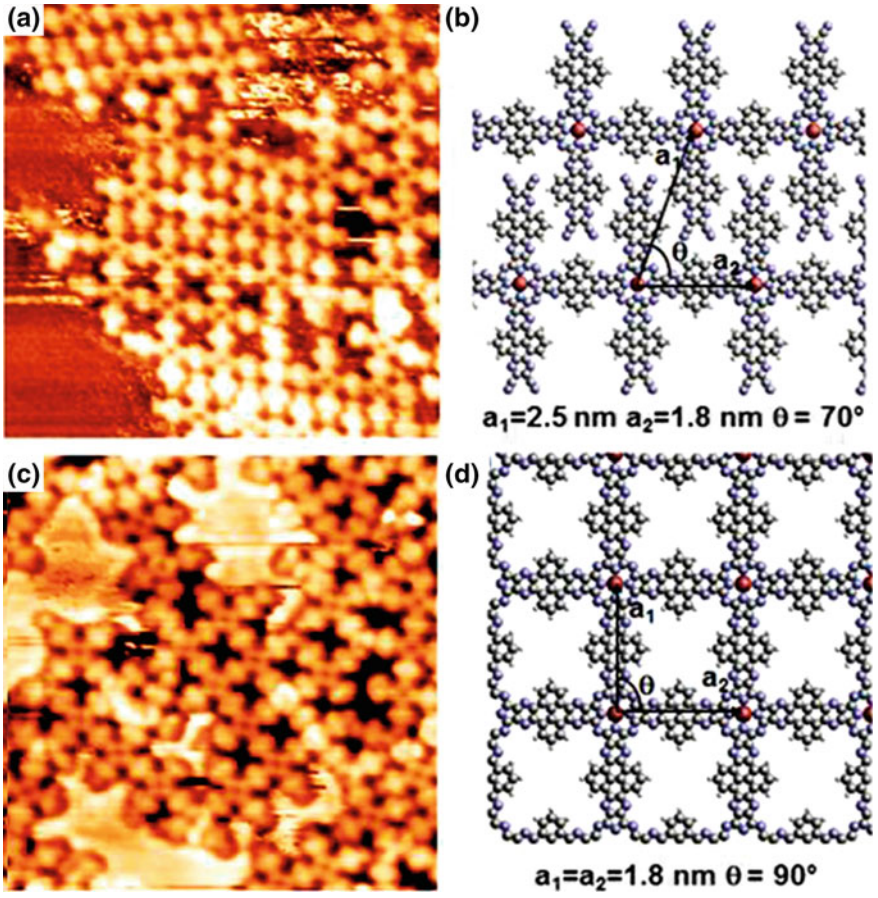

Fig. 5 Copper pyrenopyrazinocyanine (CuPyc) polymeric networks. **a** STM image (15 × 15 nm^2) of polymeric CuPyc chains, obtained by annealing the substrate at 540 K. **b** DFT model of polymeric chains. **c** STM image (15 × 15 nm^2) of the polymeric grid obtained by annealing the substrate at 675 K. **d** DFT model of polymeric grid. Adapted with permission from Ref. [14]. Copyright 2014 American Chemical Society

function of sample temperature and a new feature in the Cu2p3/2 photoemission spectrum allows a fully conclusive XPS analysis (Fig. 6). The C1s spectrum of the PPCN self-assembled network is composed of two main peaks, related to carbons of the aromatic rings (C1), carbons bonded with nitrogen atoms (C2), and a satellite of this latter (S2) [28, 29]; the C1s spectrum of the non-reacted metal–organic network (MOCN) presents the same shape slightly shifted toward higher binding energy. An evolution of the C2 peak is observed with increasing annealing temperature: Its intensity decreases and it shifts toward lower binding energy. The reaction involves the transformation of half of the carbonitrile carbons into pyrrole carbons whose binding energy is about 0.4 eV lower [30, 31]; as the reaction proceeds further to form the CuPycs, the polymeric chains, and the polymeric grid, the pyrrole component becomes more significant, thus explaining the change in the C2 peak. The Cu2p3/2 spectrum of MOCN exhibits one peak, at the same binding energy of Cu deposited on Au(111); after 475 K annealing, a new peak at about 935.4 eV appears. This value of binding energy is in good agreement with the binding energy of the Cu(II) copper peak measured for bulk CuPc and CuPc on Au

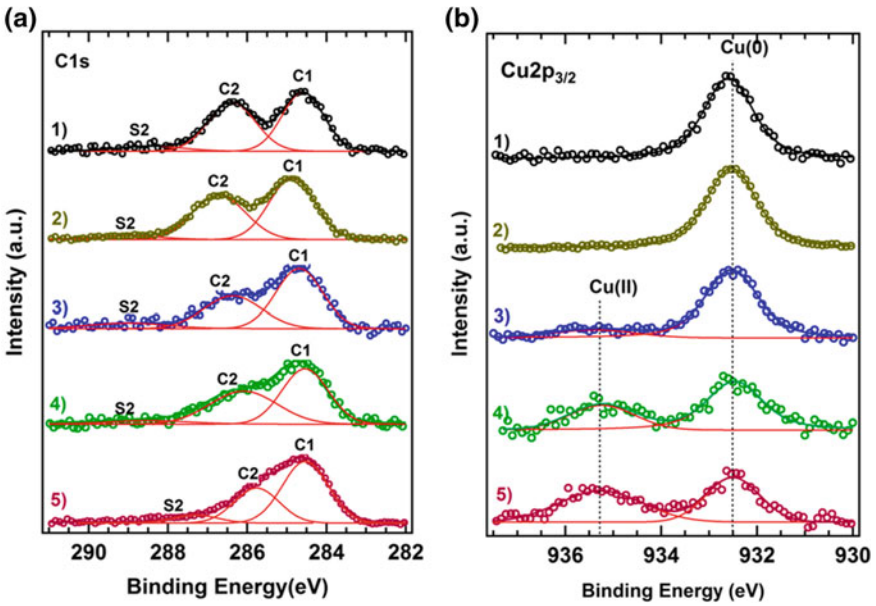

Fig. 6 X-ray photoemission spectroscopy as a function of the annealing temperature. **a** C1s spectra of, *1* PPCN self-assembled network, *2* MOCN1, *3* CuPyc coordination network (475 K annealing), *4* CuPyc polymeric chains (540 K annealing) *5* CuPyc polymeric network (675 K annealing). All the spectra were normalized to the same total area. **b** Cu2p3/2 spectra of, *1* Cu on Au(111), *2* MOCN1, *3* CuPyc coordination network (475 K annealing), *4* CuPyc polymeric chains (540 K annealing), *5* CuPyc polymeric grid (675 K annealing). All the spectra were normalized to the same total area. *Circular markers* represent the experimental data, *solid lines* the fit. The individual components of the fit are represented with *red line*. Adapted with permission from Ref. [14]. Copyright 2014 American Chemical Society

(100) [31, 32]; we interpret this peak as the signature of the CuPycs formation. Furthermore, the Cu(II):N:C ratio of the CuPyc coordination network is about 1:31:98, which is consistent with the 1:32:96 ratio of the CuPyc molecule formed on the whole surface. The intensity of the Cu(II) peak increases after 540 and 675 K annealing: this increase confirms the interpretation of the STM images and the temperature-dependent nature of the reaction, as with the formation of polymeric chains and polymeric grid more and more Cu–N bonds are indeed created.

3 Conclusion

In this chapter, we review on-surface synthesis of pi-conjugated 2D metal–organic materials, opening an access to a diversity of hybrid organic–inorganic compounds with possibly interesting transport properties. We take advantage of on-surface reaction between metallic atoms and organic precursors to confine the reaction in two dimensions. This method appeared in the last few years as a new way to form 2D materials. The choice and comparison between different molecular precursors (TCNB, PPCN) and different metallic atoms (Fe, Mn and Cu) allows us to discriminate between non-reacted and reacted species by a drastic difference in the symmetry of the self-assembled networks. Furthermore, the reaction yield obtained in the case of PPCN, close to 90 % of the surface coverage, allows a fully conclusive XPS analysis. Finally, completely new 1D and 2D pi-conjugated polymers are formed. The hierarchical synthesis of new pi-conjugated molecules embedding metals, obtained using 2D confinement of molecular precursors on surfaces, is a key step forward toward new nano-materials combining organic and inorganic species and the bottom-up production of sophisticated structures for electronic devices.

Acknowledgments We thank Dr. L. Chen, Dr. S. Clair, Dr. L. Giovanelli, Prof. X. Feng, Prof. L. Porte, and Prof. K. Muellen for fruitful discussions. This research was supported by the International Center for Frontier Research in Chemistry (Grant FRC-2010-JBu-0001). JPB thanks the Institut Universitaire de France (IUF) for support.

References

1. Leznoff, C.C., Lever A.B.P. (eds.): Phthalocyanines and related compounds, vol. 1–4.VCH, Cambridge (1996)
2. Bannehr, R., Meyer, G., Wohrle, D.: Polymer phthalocyanines and their precursors .2. the structure of polyphthalocyanines.2. Polym. Bull. **2**, 841 (1980)
3. Yudasaka, M., Nakanishi, K., Hara, T., Tanaka, M., Kurita, S., Kawai, M.: Metal phthalocyanine polymer film formation by the double source evaporation of tetracyanobenzene and metal. Synth. Met. **19**, 775 (1987)
4. Yanagi, H., Ueda, Y., Ashida, M.: Characterization of monomeric and polymeric (octacyanophthalocyaninato)metals in thin-films. Bull. Chem. Soc. Jpn. **61**, 2313 (1988)
5. Sanjai, B., Raghunathan, A., Natarajan, T.S., Rangarajan, G.: Electrical conduction in heat-treated poly metallo phthalocyanines. Mater. Sci. Eng., C **3**, 227 (1995)

6. Wöhrle, D.: Phthalocyanines in macromolecular phases – methods of synthesis and properties of the materials. Macromol. Rapid Commun. **22**, 68 (2001)
7. McKeown, N.B.: Phthalocyanine-containing polymers. J. Mater. Chem. **10**, 1979 (2000)
8. Zhou, J., Sun, Q.: Magnetism of phthalocyanine-based organometallic single porous sheet. J. Am. Chem. Soc. **133**, 15113 (2011)
9. Kezilebieke, S., Amokrane, A., Boero, M., Clair, S., Abel, M., Bucher, J.-P.: Steric and electronic selectivity in the synthesis of Fe-1,2,4,5-tetracyanobenzene (TCNB) complexes on Au(111): From topological confinement to bond formation. Nano Res. **7**, 888 (2014)
10. Abel, M., Clair, S., Ourdjini, O., Mossoyan, M., Porte, L.: Single layer of polymeric Fe-phthalocyanine: an organometallic sheet on metal and thin insulating film. J. Am. Chem. Soc. **133**, 1203 (2010)
11. Giovanelli, L., Savoyant, A., Abel, M., Maccherozzi, F., Ksari, Y., Koudia, M., Hayn, R., Choueikani, F., Otero, E., Ohresser, P., Themlin, J.-M., Dhesi, S.S., Clair, S.: Magnetic coupling and single-ion anisotropy in surface-supported Mn-based metal–organic networks. J. Phys. Chem. C **118**, 11738 (2014)
12. Kezilebieke, S., Amokrane, A., Abel, M., Bucher, J.-P.: Hierarchy of chemical bonding in the synthesis of Fe-phthalocyanine on metal surfaces: a local spectroscopy approach. J. Phys. Chem. Lett. **5**, 3175 (2014)
13. Koudia, M., Abel, M.: Step-by-step on-surface synthesis: from manganese phthalocyanines to their polymeric form. Chem. Comm. **50**, 8565 (2014)
14. Nardi, E., Chen, L., Clair, S., Koudia, M., Giovanelli, L., Feng, X., Müllen, K., Abel, M.: On-surface reaction between tetracarbonitrile-functionalized molecules and copper atoms. J. Phys. Chem. C **118**, 27549 (2014)
15. Brede, J., Atodiresei, N., Kuck, S., Lazic, P., Caciuc, V., Morikawa, Y., Hoffmann, G., Bluegel, S., Wiesendanger, R.: Spin- and energy-dependent tunneling through a single molecule with intramolecular spatial resolution. Phys. Rev. Lett. **105**, 047204 (2010)
16. Gao, L., Ji, W., Hu, Y.B., Cheng, Z.H., Deng, Z.T., Liu, Q., Jiang, N., Lin, X., Guo, W., Du, S.X., Hofer, W.A., Xie, X.C., Gao, H.J.: Site-specific Kondo effect at ambient temperatures in iron-based molecules. Phys. Rev. Lett. **99**, 106402 (2007)
17. Gopakumar, T.G., Brumme, T., Kroeger, J., Toher, C., Cuniberti, G., Berndt, R.: Coverage-driven electronic decoupling of Fe-phthalocyanine from a Ag(111) substrate. J. Phys. Chem. C **115**, 12173 (2011)
18. Heinrich, B.W., Iacovita, C., Brumme, T., Choi, D.-J., Limot, L., Rastei, M.V., Hofer, W.A., Kortus, J., Bucher, J.-P.: Direct observation of the tunneling channels of a chemisorbed molecule. J. Phys. Chem. Lett. **1**, 1517 (2010)
19. Iacovita, C., Rastei, M.V., Heinrich, B.W., Brumme, T., Kortus, J., Limot, L., Bucher, J.P.: Visualizing the spin of individual cobalt-phthalocyanine molecules. Phys. Rev. Lett. **101**, 116602 (2008)
20. Li, Z., Li, B., Yang, J., Hou, J.G.: Single-molecule chemistry of metal phthalocyanine on noble metal surfaces. Acc. Chem. Res. **43**, 954 (2010)
21. Minamitani, E., Tsukahara, N., Matsunaka, D., Kim, Y., Takagi, N., Kawai, M.: Symmetry-driven novel Kondo effect in a molecule. Phys. Rev. Lett. **109**, 086602 (2012)
22. Mugarza, A., Robles, R., Krull, C., Korytar, R., Lorente, N., Gambardella, P.: Electronic and magnetic properties of molecule-metal interfaces: transition-metal phthalocyanines adsorbed on Ag(100). Phys. Rev. B **85**, 155437 (2012)
23. Ahmadi, S., Shariati, M.N., Yu, S., Gothelid, M.: Molecular layers of ZnPc and FePc on Au (111) surface: charge transfer and chemical interaction. J. Chem. Phys. **137**, 084705 (2012)
24. Perera, U.G.E., Kulik, H.J., Iancu, V., Dias da Silva, L.G.G.V., Ulloa, S.E., Marzari, N., Hla, S.W.: Spatially extended kondo state in magnetic molecules induced by interfacial charge transfer. Phys. Rev. Lett. **105**, 106601 (2010)
25. Stepanow, S., Miedema, P.S., Mugarza, A., Ceballos, G., Moras, P., Cezar, J.C., Carbone, C., de Groot, F.M.F., Gambardella, P.: Mixed-valence behavior and strong correlation effects of metal phthalocyanines adsorbed on metals. Phys. Rev. B **83**, 220401 (2011)

26. Hammer, B., Morikawa, Y., Norskov, J.K.: CO chemisorption at metal surfaces and overlayers. Phys. Rev. Lett. **76**, 2141 (1996)
27. Norskov, J.K.: Covalent effects in the effectiveness-medium theory of chemical binding hydrogen heats of solution in the 3D metals. Phys. Rev. B **26**, 2875 (1982)
28. Lindquist, J.M., Hemminger, J.C.: High-resolution core level photoelectron spectra of solid TCNQ: determination of molecular orbital spatial distribution from localized shake-up features. J. Phys. Chem. **92**, 1394 (1988)
29. Lindquist, J.M., Hemminger, J.C.: High energy resolution X-ray photoelectron spectroscopy studies of tetracyanoquinodimethane charge transfer complexes with copper, nickel, and lithium. Chem. Mat. **1**, 72 (1989)
30. Ottaviano, L., Lozzi, L., Ramondo, F., Picozzi, P., Santucci, S.J.: Copper hexadecafluoro phthalocyanine and naphthalocyanine: the role of shake up excitations in the interpretation and electronic distinction of high-resolution X-ray photoelectron spectroscopy measurements. Electr. Spectr. Rel. Phen. **105**, 145 (1999)
31. Schwieger, T., Peisert, H., Golden, M.S., Knupfer, M., Fink, J.: Electronic structure of the organic semiconductor copper phthalocyanine and K-CuPc studied using photoemission spectroscopy. Phys. Rev. B **66**, 155207 (2002)
32. de Oteyza, D.G., El-Sayed, A., Garcia-Lastra, J.M., Goiri, E., Krauss, T.N., Turak, A., Barrena, E., Dosch, H., Zegenhagen, J., Rubio, A., Wakayama, Y., Ortega, J.E.: Copper-phthalocyanine based metal-organic interfaces: the effect of fluorination, the substrate, and its symmetry. J. Chem. Phys. **133**, 214703 (2010)